Available online at www.sciencedirect.com
SCIENCE @ DIRECT®
Journal of Crystal Growth 288 (2006) 53–56
JOURNAL OF CRYSTAL GROWTH
www.elsevier.com/locate/jcrysgro

Spatially resolved photoluminescence and Raman spectroscopy of bandgap gratings fabricated in GaAs/AlAs superlattice waveguide using quantum well intermixing

A. Saher Helmy[a,*], P. Martin[b], J.P. Landesman[b], A.C. Bryce[c], J.S. Aitchison[a], J.H. Marsh[d]

[a]*Edward S. Rodgers Department of Electrical and Computer Engineering, 10 King's college Rd., University of Toronto, Toronto, Ont., Canada M5S 3G4*
[b]*Laboratoire des Plasmas et des Couches Minces, Institut des Matériaux UMR 6502, Nantes, France*
[c]*Department of Electronics and Electrical Engineering, University of Glasgow, Glasgow G12 8QQ, UK*
[d]*Intense, Hamilton International Technology Park, Glasgow, G72 0BN, Scotland, UK*

Abstract

Photoluminescence (PL) and Raman spectroscopy were devised to study bandgap gratings fabricated in a waveguide with a core consisting of GaAs/AlAs short superlattice (SSL) structure using quantum well intermixing (QWI). The spatially resolved PL is carried out on the superlattice layer from the sample surface, as well as from a cleaved facet to the side of the epitaxial layer. The PL from the sample surface showed a modulation in the PL wavelength with shoulders being observed. The root cause of this observation was resolved via PL scans of the cleaved side of the grating. The results were further supplemented via Raman spectroscopy measurements, where Raman spectra were collected at different depths of the SSL through probing the SSL layer cross-section. SSL-related phonon states were clearly observed for the lower part of the SSL layer where intermixing did not take place, while the Raman spectra for the intermixed regions showed regular bulk phonon modes, indicating the SSL layer intermixing.

PACS: 78.30.Fs; 78.55.Cr; 78.67.−n

Keywords: A1. Optical spectroscopy; A1. Short superlattice structures; A2. Quantum well intermixing; B1. GaAs/AlAs

1. Introduction

Bandgap tailoring with lateral control of quantum confined heterostructures has moved on from enabling monolithic photonic device integration, into the realm of providing novel functionality for III–V photonics through control of non-linear and linear optical properties over the scale of one wavelength [1]. The use of second order nonlinearities in III–V semiconductors, for example, offers the possibility of efficient optical frequency conversion. Particularly in quantum confined heterostructures, where large $\chi^{(2)}$ coefficients can be obtained [2], a multitude of functional devices, ranging from integrated second harmonic generation (SHG) structures, to integrated devices for parametric generation, oscillation and amplification could be realised [3,4]. Recently, quantum well intermixing (QWI) technology has demonstrated the ability to modulate the resonant part of the second-order non-linear optical coefficients in GaAs/AlAs superlattice structures, which lead to successful quasi-phase matching and SHGs in wave guide structures with a GaAs/AlAs superlattice core [1]. A non-destructive comprehensive characterisation of such structures is essential, especially when combined with the characterisation of the efficiency of their optical non-linearity, which would then give a valuable insight into further device design. Accurate characterisation of the QPM domains is key, where it has been discovered recently that the behaviour of some QWI technologies can be drastically different depending on the feature size range [5].

Optical, and especially Photoluminescence (PL), spectroscopy are most suited for non-destructive characterisation.

*Corresponding author. Fax: +1 416 9713020.
E-mail address: a.helmy@utoronto.ca (A. Saher Helmy).

0022-0248/$ - see front matter © 2005 Published by Elsevier B.V.
doi:10.1016/j.jcrysgro.2005.12.048

PL can provide a comprehensive scan of the bandgap of a structure rapidly. Complications arise when analysing the data provided by the spatially resolved PL measurements particularly when the feature sizes measured approach those of the photo-generated carrier diffusion lengths. However, this can be circumvented, by either using other techniques such as Raman spectroscopy [6], which is not affected by carrier diffusion, or by using a carefully optimised spatially resolved PL set-up, with a spot size much smaller than the photo-generated carrier lifetime in the region studied [7]. The set-up we use in this work relies on a confocal microscope arrangement, which has the advantage of preserving the beam-waist size in the probed sample-volume. This is in contrast to conventional systems which rely on objective lenses to focus the beam. In this case, the beam will diverge once passing its focusing point, which is usually the sample surface. Therefore the resolution of the excitation beam inversely proportional to the depth of the feature studied [7].

In this paper we shall use high spatial resolution PL and Raman spectroscopy to study bandgap grating fabricated in a waveguide with a core consisting of GaAs/AlAs short superlattice. The spatially resolved spectroscopy will be carried out on the superlattice layer from the sample surface, as well as from a cleaved facet to the side of the epitaxial layer. The bandgap tuning was induced in the structures using QWI, where the technology used is based on inducing defects via SiO_2 sputtering-induced damage [8]. Waveguides made with these bandgap grating samples successfully demonstrated achieving a modulation in the non-linear optical coefficient, leading to QPM, and subsequent SHG around 1.55 μm.

2. Sample description and measurements

We shall start by describing the sample preparation. The bandgap grating in the sample was intermixed using SiO_2 sputtering-deposition induced defects. The sample is first patterned with the gratings of different periods, then sputtered SiO_2 is deposited on the surface, after which lift-off is carried out. A 200 nm thick layer of electron gun SiO_2 was then deposited. Samples were then annealed for 60 s at 725 °C with a rise time of 15 s. After removing all the remaining SiO_2, the sample is then patterned with waveguides etching, which are orthogonal to the grating direction and defined using reactive ion etching. The epitaxial structure of the samples was that of waveguide structure molecular beam eptiaxy (MBE), with a 600 nm waveguide core of 14:14 monolayer of GaAs:AlAs and a lower and upper cladding of $Al_{0.6}Ga_{0.4}As$ with thickness of 4 and 1.5 μm. The wafer had a room temperature PL wavelength of ~750 nm. Quasi-phase matching was achieved through the modulation of the non-linear coefficient $\chi^{(2)}_{zxy}$, which was realised due to the grating that has been realised in the superlattice bandgap. The bandgap gratings created had a period which ranged between approximately 5.8 and 7 μm, which corresponds to periods which were intended to achieve QPM in these waveguides between the fundamental and second harmonic at 1550 and 775 nm, respectively, in the SHG experiment [5].

The measurements were carried out using a *JY Horriba* high resolution Raman scope equipped with a sample positioning stage which has a precision XYZ mechanical system with a 0.1 μm resolution. However, the spatial resolution is still limited by the laser beam spot size, and hence the step size was kept at 0.5 μm. The laser used for probing was an Ar^+ 514 nm laser. Software was used to define and undertake the area scan; it was also to carry out the curve fitting of the data after. The properties of the curve fitted graphs can then be plotted as a function of position.

The fundamental limitations with PL measurements for such structures are best demonstrated through the measurement shown in Fig. 1, where a few PL spectra taken across one period of the grating are plotted. It is clear that at any given point on the grating there exists multiple

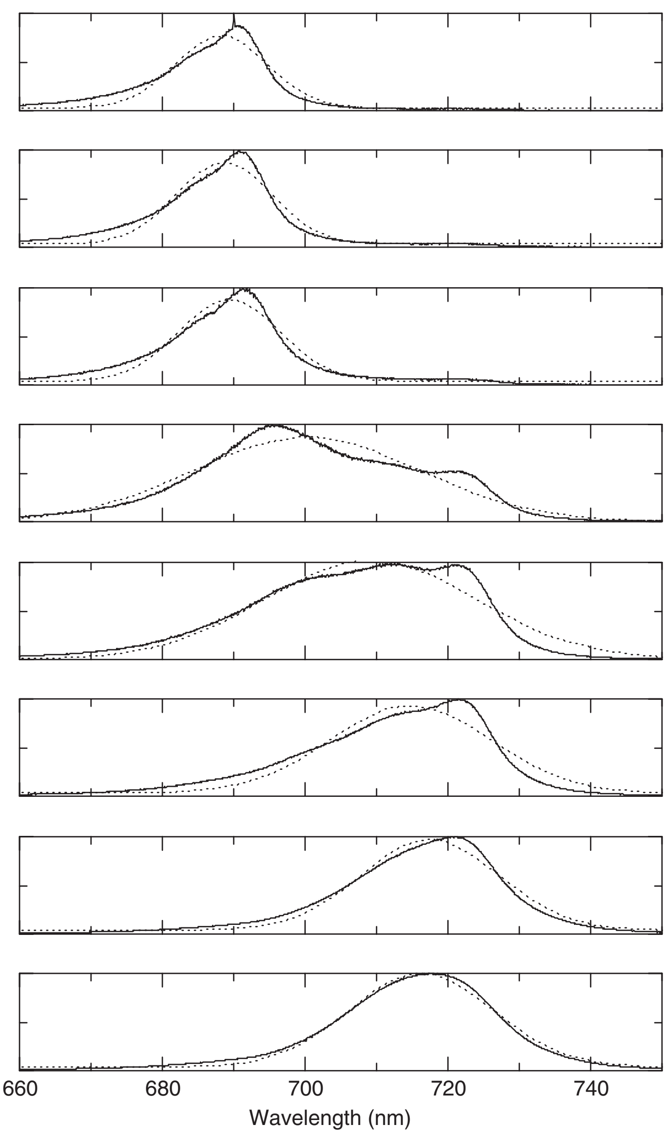

Fig. 1. PL spectra that are taken sequentially across a single period of a bandgap grating. Spectra are taken form the sample surface.

shoulders within the spectrum, which convolves the task of extracting the bandgap of the area directly illuminated by the laser. The uncertainty here arises because the spectral shoulders could be generated from the lateral photo-generated carrier diffusion from the neighbouring grating regions which may have lower bandgap [6]. Or it could indeed be generated from the rest of the short superlattice (SSL) layer which is not completely intermixed. The duty cycle is an important design tool for the nonlinear optical coefficient tailoring the in the QPM experiment [9]. It is also a parameter which can be controlled using the QWI process variables and grating mask design. A scan of the PL spectra in a 1-D scan across a few grating periods from the surface of the sample is shown in Fig. 2. Again the effects of having multiple peaks at any given point across the grating still exists in the 1D scan, however the actual duty cycle of the bandgap grating is difficult to de-convolve from such a plot as it is not known, whether the spectral shoulders arise from the depth, or the lateral photo-generated carrier diffusion. One route to over-coming this limitation in the PL measurement is to conduct a lateral scan across the bandgap grating from the cross section of the sample. However the issues with photo generated carrier diffusion from the thickness of a potential inhomogeneous the SSL layer or from the different bandgap regions of the grating would still be dominant. This is because the laser spot size excitation will generate the carries more carriers in the SSL core regions, more so than for top laser excitation [5,10].

Raman measurements have the potential of providing much higher resolution that those of the PL scans, as there is photo-generated carrier diffusion involved. However the signal to noise ratio attainable from the Raman modes of the core layer of interest is a challenge to circumvent. The Raman signal from the superlattice could not be retrieved

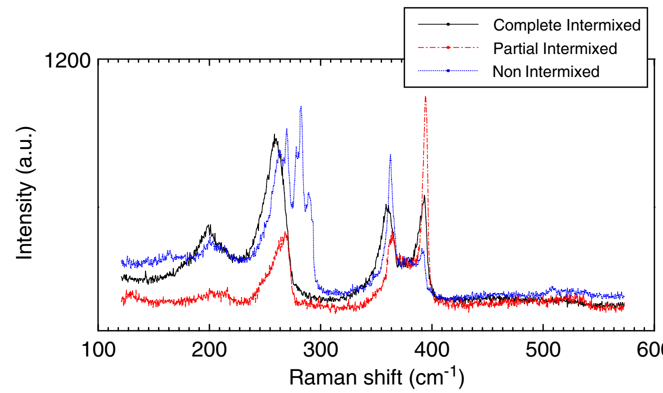

Fig. 3. Raman spectra from the SSL layer taken for spots with varying extents of intermixing. Bound (zone-folded) Raman modes are evident in the les intermixed regions, where their amplitude is larger than bulk modes.

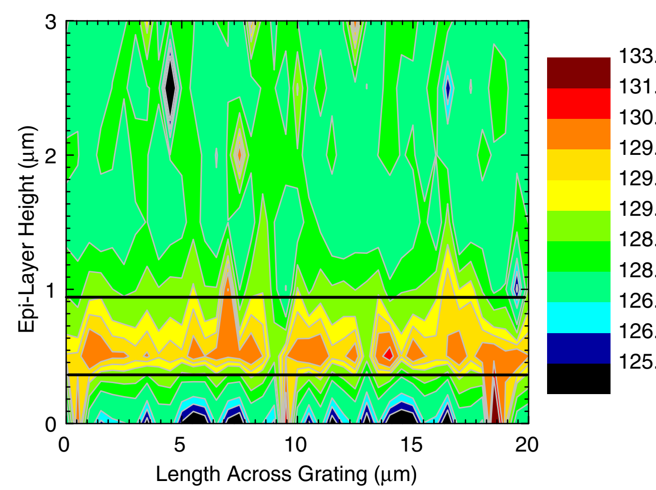

Fig. 4. The difference between the AlAs-like LO mode and the GaAs-like LO mode is plotted in a 2D map across the cross section of a few grating periods. The SSL layer is denoted by the two horizontal black lines on the graph. The incomplete intermixing in the SSL region is evident in the gradient of the ratio across the SSL layer.

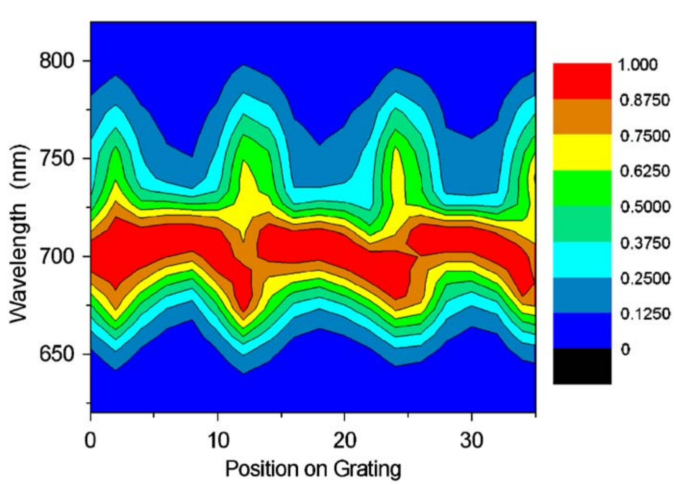

Fig. 2. PL spectra of a 1D scan across several layers of a bandgap grating. Spectra are taken form the sample surface. The asymmetric duty cycle between the intermixing enhanced and intermixing inhibited regions is evident. Yet is it not possible to ascertain whether this effect is real, or is it an artefact of the lack of complete intermixing within the depth of the SSL layer from such surface measurement.

from the surface because of absorption in the GaAs of the 514 nm laser. In Fig. 3 Raman spectra are shown for 3 spots on the SSL layer with varying extents of intermixing. Bound (zone-folded) Raman modes are evident in the les intermixed regions, where their amplitude is larger than bulk modes. From this measurement, the improvement in sensitivity of the measurement can be easily appreciated, if we elect to track the bound Raman modes instead of bulk ones to correlate the extent of intermixing of the heterostructure.

The difference between the AlAs-like LO mode and the GaAs-like LO mode are plotted in Fig. 4. In this plot the difference between both peaks is plotted in a 2-D mapped across the side of a few grating periods. The SSL core of the waveguide is indicated by the two horizontal black lines on the graph. The top of the sample is towards the top of the graph. It is interesting to observe that within the 600 nm core of the SSL layer, the amount of intermixing is more pronounced, through a higher red shift in the main

PL peak, towards the sample surface, and is less so towards the bottom. This suggest that some of the PL shoulders acquired form the top scans can be ascribed to the incomplete intermixing of SSL layer itself, and indeed has to be taken into account when establishing the duty cycle of the gratings.

3. Discussion

It must be emphasized on the outset is that the attempt of using the techniques used here is chiefly because of their non-destructive nature. The optimisation cycle is much improved when we are able to investigate bandgap gratings on the samples which we can characterize the efficiency of the non-linear interaction of. Therefore some of the solutions which could be used for the PL technique, such as masking, to improve its resolution, would defeat the purpose of the non-destructive aspect of these techniques. Side or top excitation of the gratings, also seem to lead to the of photo-generated carrier contribution to the spectra. While some work could be carried out at cryogenic temperatures to reduce the diffusion length, full width half maximum of the spectral features and hence improve the spatial resolution, the interface region will always be difficult to investigate using PL, where the bandgap gradient is largest.

Raman spectra on the other hand despite not suffering form the issues with photo-generated carrier diffusion, are difficult to collect with high signal to noise ratio values form the sample surface, and their variation versus Al composition in AlGaAs compounds is always convoluted with other effects such as stress, crystalline quality amongst other effects. Bulk-like modes for the GaAs/AlGaAs system are the most investigated within III–V compound semiconductors. However LO and TO mode dispersion behaviour with change in bandgap and hence composition is still not large enough to provide reasonable signal to noise ratio for the measurements [11]. This is signal to noise ratio is measured taken into account the spectral width of the Raman modes which is on the order of 20–40 cm^{-1} at room temperature, in comparison with the rate of change of the mode position with the Al composition [12].

One promising alternative that has become apparent in this work is utilise the quantised (zone folded) Raman modes which are specific to the SSL layer. This is due to their improved signal to noise ratio (FWHM and intensity) in comparison to other bulk modes. The difficulty to utilize such modes for characterisation of the bandgap gratings at present is the lack of understanding of their behaviour as a function of intermixing and composition change. Unlike bulk like modes, where their position is well characterized with respect to the AlGaAs composition, no similar work is available for the quantised modes. Therefore, we view the route forward is to purposefully fabricate SSL samples with varying degrees of complete intermixing and study their behaviour in order to use this in future bandgap grating characterization.

4. Conclusion

In conclusion PL and Raman spectroscopy to study bandgap grating fabricated in a waveguide with a core consisting of GaAs/AlAs short superlattice. The spatially resolved PL spectroscopy was carried out on the superlattice layer from the sample surface, as well as from a cleaved facet to the side of the epitaxial layer showed a modulation in the PL wavelength. However, the PL signal from the cleaved side of the epitaxial layer, a finite amount of the 600 nm SL layer was found to be intermixed, while the rest, which accounts to approximately to 30% of the layer, was found not completely intermixed. The results were further supplemented via Raman spectroscopy measurements, where Raman spectra were collected at different depths of the SSL through probing the SSL layer cross-section. SSL-related phonon states were clearly observed for the lower part of the SSL layer where intermixing did not take place, while the Raman spectra for the intermixed regions showed regular bulk phonon modes, indicating the SSL layer intermixing. This 3D map of the PL of the SL layer assists in drawing a clear picture of the effect the QWI has on the SSL layer, and hence optimise the device performance.

Acknowledgements

This work has been carried out under the ESPRIT project, OFCORSE II.

References

[1] A. Saher Helmy, D.C. Hutchings, T.C. Kleckner, J.H. Marsh, A.C. Bryce, J.M. Arnold, C.R. Stanley, J.S. Aitchison, C.T.A. Brown, K. Moutzouris, M. Ebrahimzadeh, Opt. Lett. 25 (2000) 1370.
[2] J.S. Aitchison, M.W. Street, N.D. Whitbread, D.C. Hutchings, J.H. Marsh, G.T. Kennedy, W. Sibbett, IEEE J. Selected Topics Quant. Electron 4 (1998) 695.
[3] J.B. Khurgin, E. Rosencher, Y.J. Ding, J. Opt. Soc. Am. B 15 (1998) 1726.
[4] E.H. Li (Ed.), Quantum Well Intermixing for Photonics, Milestone series, vol. 145, SPIE, Washington, DC, 1998.
[5] A. Saher Helmy, A.C. Bryce, C.N. Ironside, J.S. Aitchison, J.H. Marsh, S.G. Ayling, Infrared applications of semiconductors III. Symposium, Mat. Res. Soc. Symp. Proc. 607 (2000) 509.
[6] A. Saher Helmy, A.C. Bryce, C.N. Ironside, J.S. Aitchison, J.H. Marsh, Appl. Phys. Lett. 74 (1999) 3978.
[7] A. Gustafsson, M.E. Pistol, L. Montelius, L. Samuelson, J. Appl. Phys. 84 (1998) 1715.
[8] O.P. Kowalski, C.J. Hamilton, S.D. McDougall, J.H. Marsh, A.C. Bryce, R.M. De La Rue, B. Vögele, C.R. Stanley, C.C. Button, J.S. Roberts, Appl. Phys. Lett. 72 (1997) 581.
[9] D.C. Hutchings, Appl. Phys. Lett. 76 (2000) 1362.
[10] A. Saher Helmy, N.P. Johnson, M.L. Ke, A.C. Bryce, J.S. Aitchison, J.H. Marsh, I. Gontijo, G.S. Buller, J. Davidson, P. Dawson, IEEE J. Selected Topics Quant. Electronics 4 (1998) 661.
[11] S. Perkowitz, Optical Characterisation of Semiconductors, second ed, Academic Press, New York, 1994.
[12] G. Abstreiter, E. Bauser, A. Fischer, K. Ploog, Appl. Phys. 16 (1978) 345.